ISSN: 1692-7257 - Volume 2 – Number 46 - 2025

RCTA
Revista Colombiana de Tecnologías de Avanzada
UNIPAMPLONA

Digital Object Identifier: 10.24054/rcta.v2i46.3521

Method for asbestos detection in hyperspectral images using the approximate components of the wavelet transform and spectral differential similarity

Método para la detección de asbesto en imágenes hiperespectrales a partir de los componentes aproximados de la trasformada wavelet y la similitud diferencial espectral

Ph.D. Gabriel Elías Chanchí-Golondrino[1], Ph.D. Manuel Saba[1]
PhD. Manuel Alejandro Ospina-Alarcón[1]

[1] **Universidad de Cartagena,** *Facultad de Ingeniería, Cartagena, Bolívar, Colombia.*

Correspondencia: *gchanchig@unicartagena.edu.co*

Received: *january 15, 2025.* ***Accepted:*** *june 20, 2025.* ***Published:*** *july 01, 2025.*

Cómo citar: *G. E. Chanchí Golondrino, M. Saba, and M. A. Ospina Alarcón, "Method for asbestos detection in hyperspectral images based on the approximate components of the wavelet transform and spectral differential similarity", RCTA, vol. 2, no. 46, pp. 68–77, Jul. 2025.*
Recuperado de https://ojs.unipamplona.edu.co/index.php/rcta/article/view/3521

Abstract: Considering that one of the challenges in material detection within the field of hyperspectral imaging, given its high dimensionality, is the identification of more computationally efficient methods, this article proposes a method for asbestos detection based on the use of the approximate components of the wavelet transform and spectral differential similarity. Variants of the proposed method were implemented using open-source libraries, including Spectral, PyWavelets, NumPy, Pandas, and Matplotlib, achieving similar effectiveness in asbestos detection compared to the correlation-based method. Furthermore, in terms of computational efficiency, it was found that the three variants of the proposed method were more efficient than the correlation-based method, with the method based on the first component of the wavelet transform yielding the best results, being 13.964% more efficient. Based on these results, the variants of the proposed method can be considered as alternatives to conventional methods, allowing them to be integrated into systems for the analysis and monitoring of asbestos and other materials using hyperspectral images. Additionally, this study demonstrated the feasibility of using open-source tools and libraries for material identification in hyperspectral images, making this research a reference point for research centers and universities to replicate and adapt these methods in remote sensing-based investigations.

Keywords: Asbestos-cement, hyperspectral images, remote sensing, wavelet transform.

Resumen: Considerando que uno de los desafíos en la detección de materiales en el campo de las imágenes hiperespectrales ante la alta dimensionalidad, es la identificación de métodos computacionales más eficientes, en este artículo se propone como contribución un método para la detección de asbesto basado en el uso de los componentes aproximados de la transformada wavelet y la similitud diferencial espectral. Las variantes del método propuesto fueron implementadas mediante el uso de las librerías de código abierto: spectral, Pywavelets, numpy, pandas y matplotlib, obteniendo una efectividad similar en la detección de asbesto con respecto al método de la correlación. Así mismo, a nivel de la eficiencia computacional, se obtuvo que las tres variantes del método resultaron más eficientes que el método de la correlación, siendo el método basado en el primer componente de la transformada el que obtuvo los mejores resultados al ser 13.964% más eficiente. A partir de los resultados obtenidos, las variantes del método propuesto pueden ser consideradas como una alternativa a los métodos convencionales, de tal forma que pueden ser articuladas en sistemas de análisis y monitorización de asbesto y otros materiales a partir del uso de imágenes hiperespectrales. Así mismo, este trabajo demostró la factibilidad del uso de herramientas y librerías de código abierto en la identificación de materiales en imágenes hiperespectrales, por lo que esta investigación puede ser tomada como punto de referencia que centros de investigación y universidades repliquen y adapten estos métodos en investigaciones basadas en sensado remoto.

Palabras clave: Asbesto-cemento, imágenes hiperespectrales, sensado remoto, transformada wavelet.

1. INTRODUCTION

Remote sensing, also known as teledetection, can be defined as a technique aimed at acquiring information about the Earth's surface using sensors mounted on satellites, airplanes, and drones, through spectroscopic methods, that is, based on the interaction of electromagnetic energy with objects on the Earth's surface, allowing data collection without direct physical contact [1], [2], [3]. Remote sensing utilizes various regions of the electromagnetic spectrum, including visible light, infrared, and microwaves, with the purpose of recording the energy or reflectance emitted by the Earth's surface [4], [5]. Among the advantages of remote sensing is the significant reduction in time and cost associated with traditional terrestrial data collection methods, enabling the rapid acquisition of data over large areas, which is particularly beneficial for environmental monitoring and agriculture [3], [6].

One of the most widely used remote sensing techniques is hyperspectral imaging, which is based on the simultaneous acquisition of images in hundreds of narrow bands, enabling a detailed characterization of observed materials through the use of their unique spectral signatures [7], [8]. These images store data in three-dimensional structures known as datacubes, which contain spatial information (x, y) and spectral information (λ) associated with reflectance [9], [10]. In a hyperspectral datacube, each pixel has a complete spectrum or spectral signature that represents the light absorption and scattering properties of the material to which the pixel belongs [11]. While multispectral images capture data from up to ten spectral bands that are wider and non-contiguous, these bands are more limited compared to hyperspectral images, which capture reflectance data across tens to hundreds of narrow, contiguous spectral bands, providing a detailed spectrum for each pixel in the image [12], [13].

Regarding asbestos detection using hyperspectral images, various studies have been conducted. For instance, in [14], [15], hyperspectral images in the short-wave infrared range (SWIR: 1000–2500 nm) have been utilized to detect and classify asbestos materials such as amosite, crocidolite, and chrysotile in cement matrices, achieving high effectiveness with techniques like Principal Component Analysis (PCA) and Soft Independent Modeling of Class Analogies (SIMCA). Similarly, in [16], [17], supervised learning models based on Support Vector Machines (SVM) and Partial Least Squares Regression (PLSR) have been effectively employed for identifying asbestos-containing materials in construction and demolition waste, demonstrating their potential as a promising quality control strategy. Furthermore, in [18], a dynamic neural network model was developed to identify asbestos roofs using hyperspectral images in urban and rural areas covering up to 8,000 kilometers. Additionally, in [19], convolutional neural networks were applied to a dataset of hyperspectral images from Poland to identify fiber cement roofs, achieving an accuracy exceeding 90%.

From the above, it is evident how machine learning models and neural networks have gained prominence due to their effectiveness in detecting asbestos in hyperspectral images. Despite this, one of the challenges faced by these models in the context of hyperspectral images is the computational capacity required to process the considerable volume of data, resulting from the hundreds of spectral bands these images contain [8]. In the same vein, the complexity of machine learning models increases with the dimensionality of the data, which can lead to issues such as overfitting and the need for dimensionality reduction techniques [20], [21]. Thus, there is a need for alternative methods with lower complexity that demand fewer computational resources while achieving effectiveness comparable to that of widely used methods, such as those based on machine learning and correlation.

This article proposes, as a contribution, an alternative mathematical method for the detection of asbestos-cement in hyperspectral images, based on the use of the levels of the approximate components of the Haar wavelet transform and the spectral differential similarity method. The wavelet transform was employed to obtain a summarized version of both the spectral signature of asbestos-cement and the signature of the various pixels in the image, which were then used to calculate the spectral similarity between the approximate components and determine the potential classification of an image pixel (asbestos or non-asbestos). The wavelet transform enables the decomposition of a signal into components at different scales, with the approximation component being responsible for the global information of the signal [22] and crucial in applications requiring a multiresolution representation of the signal [23]. The approximation component is obtained by applying a low-frequency filter to the original signal, resulting in a representation that preserves the essential information of the signal at a broader scale [24]. The process of decomposing the signal into its various components is performed hierarchically, allowing the signal to be analyzed at different levels of resolution [25]. In this study, the first, second, and third hierarchical levels of the approximation component were utilized to evaluate the effectiveness of the proposed method.

The proposed method, along with its different variants (different hierarchical levels of the transform), was evaluated against the correlation method, which is one of the most widely used approaches for material detection in the field of hyperspectral imaging [26]. It is worth mentioning that the proposed method was implemented using open-source libraries and technologies, such as Spectral, PyWavelets, NumPy, Pandas, and Matplotlib, enabling its extrapolation to academic and industrial contexts for the analysis and detection of asbestos and other materials in hyperspectral images. Given the results obtained in terms of effectiveness and efficiency, the method can be integrated into automated systems for the detection of various types of materials. Finally, this method is of significant relevance in the context of Colombia, as it facilitates asbestos detection and the prioritization of interventions in specific urban areas, considering the health impacts of asbestos, including pulmonary diseases such as asbestosis and mesothelioma [27], [28], [29].

The remainder of the article is organized as follows: Section 2 presents the methodological phases considered for the development of this research. Section 3 details the results obtained, including, in the first instance, the determination of the first three levels of the approximate components of the wavelet transform associated with the spectral signature of asbestos cement. This section also includes the implementation and evaluation of the three methods (one for each component) using sample pixels of asbestos and non-asbestos, aiming to identify the minimum detection thresholds for asbestos for each component. Similarly, using the thresholds identified for each component, this section presents the application of the three methods to the complete image to determine the percentage of asbestos detected by each method. Additionally, this section evaluates the effectiveness and efficiency of each method compared to the correlation method. Finally, Section 4 presents the conclusions and future work derived from this research.

2. METHODOLOGY

For the development of this research, five methodological phases were defined as follows: P1. Selection of sample pixels for asbestos and other materials, P2. Determination of the characteristic pixel for asbestos, P3. Implementation and evaluation of the method variants using asbestos and other material pixels, P4. Application of the method variants to the reference image, and P5. Evaluation of the effectiveness and efficiency of the method variants compared to the correlation method.

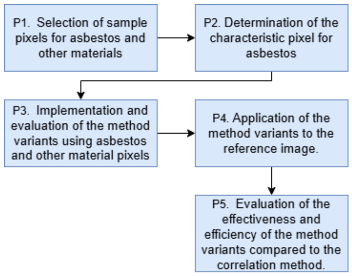

Fig. 1. *Methodology considered.*
Source: *own elaboration.*

In Phase 1 of the methodology, a set of 75 asbestos pixels and 75 pixels from other materials were selected from a reference hyperspectral image of 725x850 pixels, with 380 reflectance bands per pixel, corresponding to a representative area of the Manga neighborhood in the city of Cartagena de Indias. Thus, Figure 2 presents an RGB representation of the hyperspectral image, where the 75 selected asbestos pixels are highlighted in green, and the 75 pixels from other materials are highlighted in blue.

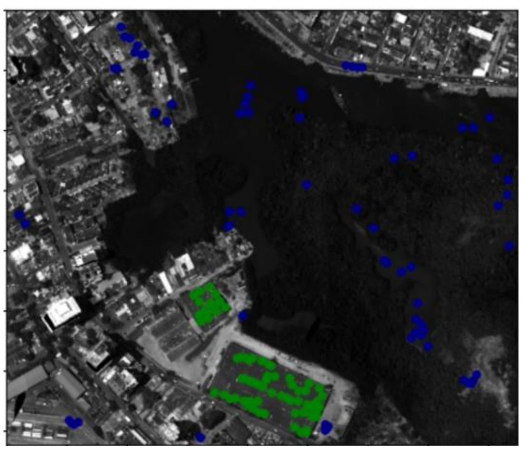

Fig. 2. *Pixels selected from asbestos and other materials.*
Source: *own elaboration.*

It is worth mentioning that these sample pixels were selected to identify the detection thresholds for each variant of the proposed method. In Phase 2 of the methodology, the characteristic pixel for asbestos-cement was determined by calculating the band-by-band average of the normalized reflectance of the 75 sample pixels, resulting in the characteristic curve that enables the differentiation of asbestos from other materials. Accordingly, Figure 3 presents the normalized spectral curve of the 75 asbestos pixels and the characteristic pixel obtained from these sample pixels.

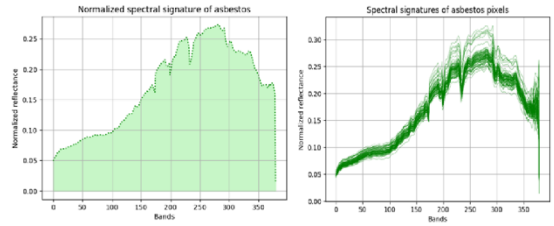

Fig. 3. *Characteristic spectral signature of asbestos-cement.*
Source: *own elaboration.*

Once the characteristic spectral signature of asbestos-cement was obtained, Phase 3 of the methodology began with the calculation of the approximate components corresponding to the first three levels of the Haar wavelet transform. These components provide a summarized representation of the characteristic pixel, where each component of the transform represents a signature with half the number of bands of the previous level. Using each of the three summarized spectral signatures, an iteration was performed over the 75 asbestos pixels and 75 non-asbestos pixels. For each pixel, the corresponding wavelet transform at the level of the spectral signature used was calculated, and the spectral similarities between the approximate components of each pixel and the spectral signature were determined using spectral differential similarity. This process aimed to identify, for each signature, the minimum similarity percentage with asbestos pixels and the maximum similarity percentage with pixels of other materials. Thus, for the calculation of the wavelet transform of the characteristic pixel, as well as for each sample pixel at its different levels, an adaptation of Equation (1) was used, which corresponds to the first level of the approximate component. It can be noted that, since the Haar transform operates on consecutive pairs, the value of i in the equation varies up to 190, which is half of 380.

$$A_i = \frac{r_{2i-1} + r_{2i}}{\sqrt{2}}, i = 1, .., 190 \quad (1)$$

On the other hand, the similarity between the approximate components of the spectral signature and each pixel was calculated using Equation (2), which determines the percentage of spectral similarity between the components [30].

$$sim = 100 - \frac{\sum_{i=1}^{n} \left| pix_i - pix_{prom} \right|}{n} x\, 100 \quad (2)$$

Once the minimum similarity percentage with asbestos and the maximum similarity percentage with non-asbestos pixels were detected for each of the three levels of the wavelet transform, Phase 4 of the methodology proceeded with the application of the three variants of the method to the complete image, obtaining in each case the percentage of asbestos pixels corresponding to the reference image.

Finally, in Phase 5, the percentages obtained by each of the three variants of the method were compared with the percentage of asbestos detected using the correlation method, which has been widely applied in the detection of materials in hyperspectral images. Additionally, this phase included the evaluation of the efficiency of the three method variants in comparison to the correlation method. To achieve this, all four methods were executed a total of 100 times on a region of the reference image measuring 20x20 pixels, with each pixel containing 380 reflectance bands. For each method, the average processing time for the image was obtained, and an effectiveness ranking was conducted, identifying the method with the best performance in terms of both effectiveness and efficiency relative to the correlation method.

3. RESULTS AND DISCUSSION

Firstly, in terms of results, the approximate components of the wavelet transform for the first three levels were obtained from the characteristic or average asbestos pixel (see Figure 3). These components are presented in Figure 4, along with the original spectral signature. From Figure 4, it is evident that the original spectral signature consists of 380 reflectance bands, which are halved with each of the three approximate components of the Haar wavelet transform. Thus, while the overall shape of the spectral signature is preserved, the first component contains 190 bands, the second component has 95 bands, and the third component consists of 48 bands.

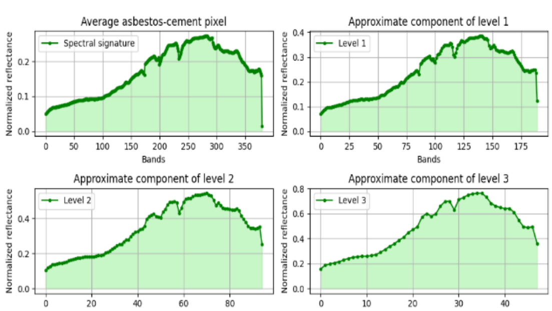

Fig. 4. *First three levels of the approximate component.*
Source: *own elaboration.*

As mentioned in the methodology, each of the first three components was used to evaluate the asbestos detection capability using the 75 asbestos pixels and the 75 non-asbestos pixels. For each of the three components, the minimum spectral similarity percentage with asbestos pixels and the maximum spectral similarity percentage with pixels of other materials were determined with respect to the corresponding summarized spectral signature. As an example, Figure 5 presents the detected thresholds for each level of the components of the Haar wavelet transform.

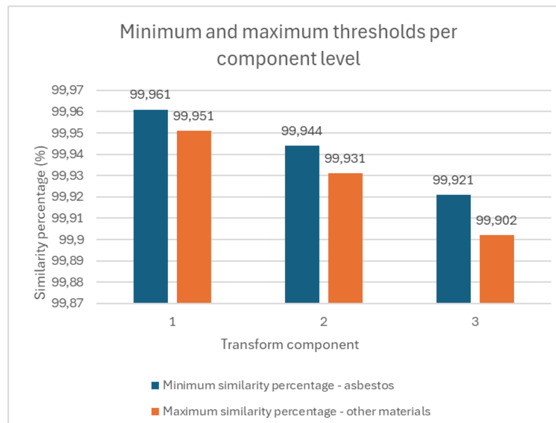

Fig. 5. *Minimum and maximum thresholds per component level.*
Source: *own elaboration.*

According to the results presented in Figure 5, it can be observed that, across the three different levels of the approximate component, there are no overlaps between the minimum similarity percentage with asbestos and the maximum similarity percentage with other materials. Furthermore, it is evident that as the component level increases, or the spectral signature of asbestos becomes more summarized, the minimum detection percentage decreases, and the difference between the two thresholds increases. Thus, while the difference between the thresholds for the first-level component is 0.01, it increases to 0.019 for the third-level component.

Once the thresholds for the three variants of the method were identified, the next step was to apply them to the entire reference image. For each pixel in the image, the respective level of the approximate component was computed for each method, and its similarity to the spectral signature associated with that level was determined. Each pixel was then classified as asbestos or non-asbestos based on the threshold described in Figure 5. As an example, Figure 6 illustrates both the application of the method for the first component of the transform on the reference image and the resulting detection, where the detected asbestos pixels are highlighted in

ISSN: 1692-7257 - Volume 2 – Number 46 - 2025

blue. From the above, it is important to note that as the component level increases, while the recursive calculations also increase, there is a lower likelihood of the method misclassifying asbestos pixels as those of other materials.

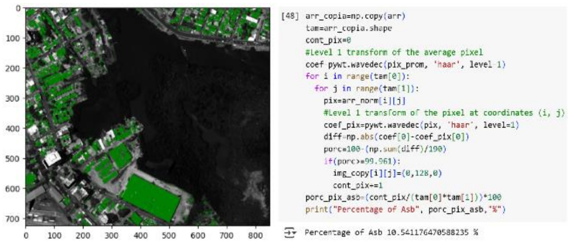

Fig. 6. *Asbestos pixels detected for the first approximate component.*
Source: *own elaboration.*

In the same manner as the method was applied using the first component on the complete image, it was adapted for the second and third components, adjusting the respective detection thresholds in each case. Thus, for each variant of the method, a percentage of asbestos detected across the entire image was obtained, which was then compared with the percentage of asbestos detected by the correlation method, following the determination of detection thresholds for that method. Accordingly, Figure 7 presents the implementation of the correlation method on the complete image, using a minimum detection threshold of 99.369% for correlation.

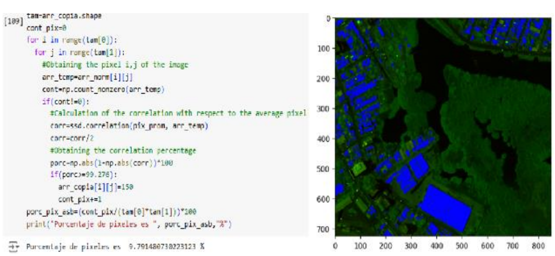

Fig. *7. Asbestos pixels detected by the correlation method.*
Source: *own elaboration.*

Similarly, Figure 8 presents the percentages of asbestos detected by each of the methods considered, in comparison with the correlation method. It can be observed that all four methods detect an asbestos percentage in the image close to 10%, with the method based on the level 1 component being the closest to the percentage detected by the correlation method, showing a percentage difference of 1.072%. Despite this, the largest difference from the correlation method is only 1.229% and corresponds to the method based on the level 3 component. Thus, it can be concluded that the three method variants, in terms of effectiveness, produce results consistent with the correlation method and can be considered viable alternatives.

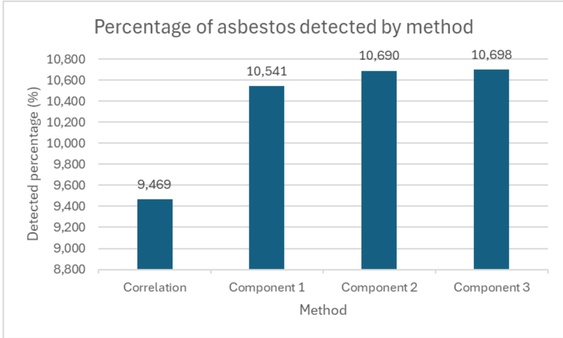

Fig. 8. *Percentage of asbestos detected by each method.*
Source: *own elaboration.*

To evaluate the efficiency of the three variants of the method compared to the correlation method, 100 executions of the four methods were performed on a region of the reference image measuring 20x20 pixels, each containing 380 reflectance bands. These evaluations were conducted using Python's timeit library in a standard cloud environment on Google Colab, with 12.67 GB of available RAM. For each method, the average processing time for the image region across 100 executions was calculated, with the results presented in Figure 9.

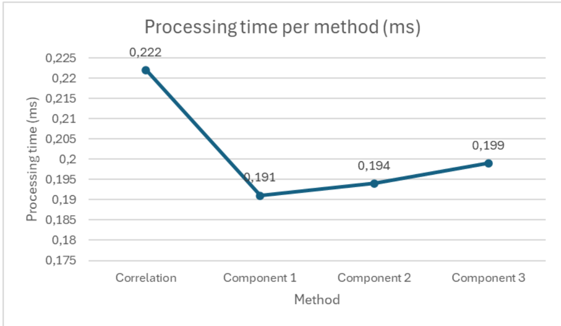

Fig. 9. *Processing time obtained by method.*
Source: *own elaboration.*

According to the results presented in Figure 9, it can be observed that the processing times of the methods are similar, ranging from 0.191 ms to 0.222 ms, with all three methods based on different levels of the approximate component achieving better performance than the correlation method. Furthermore, it is evident that the method based on the first-level approximate component achieves the best processing time at 0.191 ms. By comparing the processing times of each method, it is possible to calculate the efficiency percentage relative to the correlation method, as shown in Figure 10.

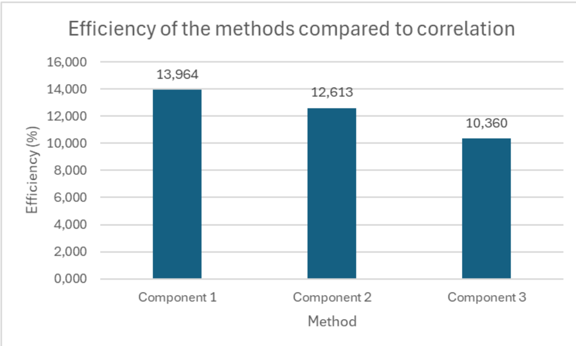

Fig. 10*. Efficiency of the methods compared to the correlation method.*
Source: *own elaboration.*

According to the results shown in Figure 10, it can be observed that the method based on the first component of the Wavelet transform achieves the best results, with a 13.964% increase in efficiency. This can be explained by the fact that calculating a greater number of components involves additional recursive computations. However, given the efficiency and effectiveness results, any of the three methods considered can be regarded as a viable alternative to the correlation method.

This article proposed a novel method for asbestos detection in hyperspectral images, based on the use of the first three levels of the approximate components of the Haar wavelet transform. The method demonstrated, through its different variants, a similar capability for detecting asbestos-cement and superior computational performance compared to the correlation method, which has been widely applied in material detection in hyperspectral images [26]. In this context, based on the efficiency results and considering the complexity of machine learning models for processing large-scale hyperspectral images [20], [21], the proposed method represents a suitable alternative for integration into systems for material detection and monitoring using hyperspectral images in urban areas. Finally, given the use of open-source libraries and technologies for the method's implementation and evaluation, this work demonstrates the feasibility of utilizing these technologies for material detection in hyperspectral images. This enables the replication of these methods and their variations in academic and industrial settings, addressing the high costs associated with proprietary tools for processing such images.

4. CONCLUSIONS

Driven by the need for more efficient methods with accuracy comparable to conventional approaches for material detection, specifically asbestos-cement, this study proposed a novel method for asbestos detection based on the levels of the wavelet approximation component and spectral differential similarity. The proposed method demonstrated effectiveness equivalent to the correlation method while achieving superior computational efficiency. Consequently, the proposed method can be considered a viable alternative for integration into systems for monitoring and tracking materials in hyperspectral images.

When comparing the three variants of the proposed method, based on the first three approximate components of the wavelet transform, to the correlation method, it was found that the different variants detected a percentage of asbestos similar to that detected by the correlation method in the reference hyperspectral image. The largest difference from the correlation method was only 1.229% and corresponded to the method based on the third component of the wavelet transform. Similarly, the variant with the smallest difference was the one based on the third component of the wavelet transform, with a percentage difference of 1.072%. These results allow us to conclude that the method's variants can be considered a viable alternative to the correlation method for detecting asbestos and other materials.

In terms of the computational efficiency of the implemented method variants, it was found that after performing 100 executions of these variants and the correlation method on a hyperspectral image of 20x20 pixels with 380 reflectance bands, the three variants demonstrated better efficiency than the correlation method, being between 10.360% and 13.964% more efficient. Among these, the method based on the first component achieved the best results. This is due to the fact that calculating a greater number of components involves additional recursive computations. Thus, the method variants can be considered a viable alternative for processing large-scale hyperspectral images, such as those obtained through remote sensing in rural areas, where efficient processing of large data volumes is required.

Based on the results obtained in this study, it can be concluded that the method based on the first component of the wavelet transform achieves detection effectiveness similar to that of the correlation method while being 13.964% more efficient. This makes it the best option to consider for asbestos-cement detection in hyperspectral images. It is worth noting that this method utilizes a spectral signature that, compared to the original, reduces the number of bands by half, using 190 bands instead of 380.

For the development of this research, open-source libraries and technologies were utilized, proving effective for the processing and analysis of hyperspectral images in the context of asbestos-cement detection. Specifically, the Spectral library facilitated access to the reflectance band data of the hyperspectral image as NumPy arrays; the PyWavelets library enabled the determination of the Haar wavelet transform components for both the spectral signature of asbestos and the image pixels; the NumPy library supported the handling of reflectance data from the image and the implementation of the spectral differential similarity method; the Pandas library allowed for the loading of coordinates corresponding to the 75 asbestos sample pixels and the 75 pixels from other materials; and the Matplotlib library facilitated the generation of graphs associated with the original spectral signature of asbestos and its summarized version (derived from the transform components). These libraries can thus be highly valuable for replicating the experiments conducted in this study or for detecting other materials in hyperspectral images, especially given the high costs associated with proprietary software typically used for analyzing such images.

As future work derived from this research, the proposed methods will first be evaluated for detecting various materials in environmental contexts, such as vegetation, water bodies, and others. Additionally, a new experimental dataset will be developed based on the summarized spectral signatures of a representative sample of pixels from the reference image, utilizing the wavelet transform. Using this new dataset, the aim is to assess the effectiveness and efficiency of machine learning-based methods for asbestos detection.

ACKNOWLEDGMENTS

The authors of this research express their gratitude to the University of Cartagena for the support provided during the development of this study.

REFERENCES

[1] J. Awange and J. Kiema, “Fundamentals of Remote Sensing,” 2019, pp. 115–123. doi: 10.1007/978-3-030-03017-9_7.

[2] A. F. Jiménez-López, M. Jiménez-López, and F. R. Jiménez-López, “Multispectral analysis of vegetation for remote sensing applications,” *ITECKNE*, vol. 12, no. 2, Nov. 2015, doi: 10.15332/iteckne.v12i2.1242.

[3] A. A. Misra, “Remote Sensing Fundamentals,” in *Atlas of Structural Geological and Geomorphological Interpretation of Remote Sensing Images*, Wiley, 2022, pp. 7–14. doi: 10.1002/9781119813392.ch1.

[4] C. Nansen and N. Elliott, “Remote Sensing and Reflectance Profiling in Entomology,” *Annu. Rev. Entomol.*, vol. 61, no. 1, pp. 139–158, Mar. 2016, doi: 10.1146/annurev-ento-010715-023834.

[5] R. Navalgund, V. Jayaraman, and P. Roy, “Remote sensing applications: An overview,” *Curr. Sci.*, vol. 93, pp. 1747–1766, 2007.

[6] B. Verma, M. Porwal, A. K. Jha, R. G. Vyshnavi, A. Rajpoot, and A. K. Nagar, “Enhancing Precision Agriculture and Environmental Monitoring Using Proximal Remote Sensing,” *J. Exp. Agric. Int.*, vol. 45, no. 8, pp. 162–176, Jul. 2023, doi: 10.9734/jeai/2023/v45i82168.

[7] W. M. Castro Silupu, I. J. Yoplac Tafur, and C. A. López Portocarrero, “Predicción del color y contenido de humedad en café cerezo mediante redes neuronales y regresión de mínimos cuadrados parciales,” *Cienc. Amaz.*, vol. 5, no. 2, p. 91, Dec. 2015, doi: 10.22386/ca.v5i2.94.

[8] M. E. Paoletti, J. M. Haut, J. Plaza, and A. Plaza, “Estudio Comparativo de Técnicas de Clasificación de Imágenes Hiperespectrales,” *Rev. Iberoam. Automática e Informática Ind.*, vol. 16, no. 2, p. 129, Mar. 2019, doi: 10.4995/riai.2019.11078.

[9] L. Gao and R. T. Smith, “Optical hyperspectral imaging in microscopy and spectroscopy - a review of data acquisition,” *J. Biophotonics*, vol. 8, no. 6, pp. 441–456, Jun. 2015, doi: 10.1002/jbio.201400051.

[10] B. Park, “Future Trends in Hyperspectral Imaging,” *NIR news*, vol. 27, no. 1, pp. 35–38, Feb. 2016, doi: 10.1255/nirn.1583.

[11] J. Burger and A. Gowen, “Data handling in hyperspectral image analysis,” *Chemom. Intell. Lab. Syst.*, vol. 108, no. 1, pp. 13–22, Aug. 2011, doi:

10.1016/j.chemolab.2011.04.001.

[12] S. Muhammed*, R. D, and V. S, "Hyperspectral and Multispectral Image Fusion Techniques," *Int. J. Recent Technol. Eng.*, vol. 8, no. 5, pp. 467–471, Jan. 2020, doi: 10.35940/ijrte.E4904.018520.

[13] H. González-Núñez and R. de la Fuente, "Offner imaging spectrometers," *Opt. Pura y Apl.*, vol. 50, no. 1, pp. 37–47, Mar. 2017, doi: 10.7149/OPA.50.1.49506.

[14] G. Bonifazi, G. Capobianco, and S. Serranti, "Asbestos containing materials detection and classification by the use of hyperspectral imaging," *J. Hazard. Mater.*, vol. 344, pp. 981–993, Feb. 2018, doi: 10.1016/j.jhazmat.2017.11.056.

[15] G. Bonifazi, G. Capobianco, and S. Serranti, "Hyperspectral imaging applied to the identification and classification of asbestos fibers," in *2015 IEEE SENSORS*, IEEE, Nov. 2015, pp. 1–4. doi: 10.1109/ICSENS.2015.7370458.

[16] G. Bonifazi, G. Capobianco, S. Serranti, S. Malinconico, and F. Paglietti, "ASBESTOS DETECTION IN CONSTRUCTION AND DEMOLITION WASTE ADOPTING DIFFERENT CLASSIFICATION APPROACHES BASED ON SHORT WAVE INFRARED HYPERSPECTRAL IMAGING," *Detritus*, no. 20, pp. 90–99, Aug. 2022, doi: 10.31025/2611-4135/2022.15211.

[17] G. Bonifazi, G. Capobianco, and S. Serranti, "Hyperspectral Imaging and Hierarchical PLS-DA Applied to Asbestos Recognition in Construction and Demolition Waste," *Appl. Sci.*, vol. 9, no. 21, p. 4587, Oct. 2019, doi: 10.3390/app9214587.

[18] D. Gubiani *et al.*, "A dynamic neural network model for the identification of asbestos roofings in hyperspectral images covering a large regional area," *Comput. Civ. Infrastruct. Eng.*, Nov. 2024, doi: 10.1111/mice.13376.

[19] M. Krówczyńska and E. Wilk, "Identification of asbestos-cement roofing with the use of remote sensing data in the capital city of Poland," *Int. Arch. Photogramm. Remote Sens. Spat. Inf. Sci.*, vol. XLVIII-3–2, pp. 273–278, Nov. 2024, doi: 10.5194/isprs-archives-XLVIII-3-2024-273-2024.

[20] Y. Chen, H. Jiang, C. Li, X. Jia, and P. Ghamisi, "Deep Feature Extraction and Classification of Hyperspectral Images Based on Convolutional Neural Networks," *IEEE Trans. Geosci. Remote Sens.*, vol. 54, no. 10, pp. 6232–6251, Oct. 2016, doi: 10.1109/TGRS.2016.2584107.

[21] J. Torres Tello, "Aprendizaje profundo para predicciones que usan imágenes multiespectrales en agricultura," *ConcienciaDigital*, vol. 6, no. 4.1, pp. 75–87, Oct. 2023, doi: 10.33262/concienciadigital.v6i4.1.2734.

[22] M. Unser and T. Blu, "Wavelet theory demystified," *IEEE Trans. Signal Process.*, vol. 51, no. 2, pp. 470–483, Feb. 2003, doi: 10.1109/TSP.2002.807000.

[23] G. C.-H. Chuang and C.-C. J. Kuo, "Wavelet descriptor of planar curves: theory and applications," *IEEE Trans. Image Process.*, vol. 5, no. 1, pp. 56–70, Jan. 1996, doi: 10.1109/83.481671.

[24] Y. Tounsi, A. Ghlaifan, M. Kumar, F. Mendoza-Santoyo, O. Matoba, and A. Nassim, "Fringe Pattern Analysis in Wavelet Domain," in *Holographic Materials and Applications*, IntechOpen, 2019. doi: 10.5772/intechopen.87943.

[25] R. Ohura and T. Minamoto, "A blind digital image watermarking method based on the dyadic wavelet packet transform and fast interval arithmetic techniques," *Int. J. Wavelets, Multiresolution Inf. Process.*, vol. 13, no. 05, p. 1550040, Sep. 2015, doi: 10.1142/S021969131550040X.

[26] G. E. Chanchí Golondrino, M. A. Ospina Alarcón, and M. Saba, "Vegetation Identification in Hyperspectral Images Using Distance/Correlation Metrics," *Atmosphere (Basel).*, vol. 14, no. 7, p. 1148, Jul. 2023, doi: 10.3390/atmos14071148.

[27] M. Kottek and M. L. Yuen, "Public health risks from asbestos cement roofing," *Am. J. Ind. Med.*, vol. 65, no. 3, pp. 157–161, Mar. 2022, doi: 10.1002/ajim.23321.

[28] M. Krówczyńska and E. Wilk, "Environmental and Occupational Exposure to Asbestos as a Result of Consumption and Use in Poland," *Int. J. Environ. Res. Public Health*, vol. 16, no.

14, p. 2611, Jul. 2019, doi: 10.3390/ijerph16142611.

[29] C. A. Saito *et al.*, "Sex-Specific Mortality from Asbestos-Related Diseases, Lung and Ovarian Cancer in Municipalities with High Asbestos Consumption, Brazil, 2000–2017," *Int. J. Environ. Res. Public Health*, vol. 19, no. 6, p. 3656, Mar. 2022, doi: 10.3390/ijerph19063656.

[30] G. Chanchí-Golondrino, M. Ospina-Alarcón, and M. Saba, "Propuesta de un método computacional para la detección de asbesto en imágenes hiperespectrales a partir de la similitud diferencial espectral," *Rev. Colomb. Tecnol. Av.*, vol. 1, no. 45, pp. 195–203, 2025.